Acta of Bioengineering and Biomechanics
Vol. 16, No. 2, 2014

Original paper
DOI: 10.5277/abb140207

Investigation of the biomechanical behaviour of articular cartilage in hindfoot joints

CHIARAVENTURATO*, PIERO GIOVANNI PAVAN, ANTONELLA FORESTIERO, EMANUELE LUIGI CARNIEL, ARTURO NICOLA NATALI

University of Padova, Centre of Mechanics of Biological Materials, Padova, Italy.

Numerical models represent a powerful tool for investigating the biomechanical behavior of articular cartilages, in particular in the case of complex conformation of anatomical site. In the literature, there are complex non-linear-multiphase models for investigating the mechanical response of articular cartilages, but seldom implemented for the analysis of high organized structure such as the foot. In the present work, the biomechanical behavior of foot cartilage is investigated by means of a fiber-reinforced hyperelastic constitutive model. The constitutive parameters are obtained through the comparison between *in vitro* experimental indentation tests on cartilage and numerical analysis data interpreting the specific experimental conditions. A finite element model of the hindfoot region is developed. Particular attention is paid to model cartilage in order to respect its morphometric configuration, including also the synovial capsule. The reliability of the procedure adopted is evaluated by comparing the numerical response of tibio-talar joint model with in vivo experimental tests mimicking the foot response in stance configuration.

Key words: *ankle joint, articular cartilage, constitutive model, numerical analysis*

1. Introduction

Articular cartilages are a hierarchically organized tissue and have the important role to resist and distribute compressive and shear loads, providing a bearing surface with low friction [1], thus protecting the underlying bone from ribbing with the other bones involved in the joint [2]. For the fundamental function performed in human movements and the particularly complex structural conformation, the mechanical behaviour of cartilaginous tissue is of high interest. The constitutive models proposed for its characterization are often very sophisticated, as multiphase models with a high number of parameters to be defined by means of experimental tests that prove to be very difficult to execute.

With concern to the histological aspect, articular cartilage is a specialized connective tissue composed of an extra-cellular matrix and a cellular part. The extra-cellular matrix is formed of a solid that includes proteoglycans and a fiber net of collagen and elastin. The fibres are embedded in interstitial fluid that is composed prevalently of water in a quantity of 70–85% of cartilage weight [3]. The content and the organization of cartilage components vary within the thickness of the tissue [4]. The particular organization is optimized depending on the function developed and leads to the definition of four zones from the upper surface to the subchondral bone: tangential, medial, deep and subchondral zone. On the tangential zone collagen fibres are organized parallel to the articular surface and radially distributed. This configuration is aimed at the proper response to compressive load and shear stress [5], [6]. Moreover the minimum wear is provided by the interaction of synovial fluid and the smooth articular cartilage surface [7]. The articular lined bone ends are enclosed by the fibrous capsule and inner synovial lining [8].

* Corresponding author: Chiara Venturato, University of Padova, Centre for Mechanics of Biological Materials, Via F. Marzolo 9, I-35131 Padova (Italy). Tel: +39 (0)49 827 5605, fax +39 (0)49 827 5604, e-mail: chiara.venturato@unipd.it

Received: December 18th, 2012
Accepted for publication: September 23rd, 2013

In order to define the mechanical response related to microstructural and histological properties of articular cartilage, complex constitutive models are proposed in the literature. These models are capable to describe with high detail the properties of cartilage and to consider the components involved in the mechanical response, such as cells, fibers, water molecules and ions charges. For this purpose, linear transversely isotropic biphasic [9], poroelastic [10], poroviscoelastic [11]–[13], fiber-reinforced poroelastic [14]–[16], fiber-reinforced poroviscoelastic [17], biphasic visco-hyperelastic fiber-reinforced [18] and fiber-reinforced poroviscoelastic swelling [19], [20] models are introduced to simulate more and more realistically the composite structure of articular cartilage. In detail they capture accurately the time-dependent mechanical behavior under loading due to its matrix composition and fiber organization. These constitutive models are used in numerical analysis to reproduce experimental conditions of confined and unconfined compressive tests, as well as indentation tests on cartilage disk samples [9], [20]–[22]. Actually, most numerical models associated with complex geometries of hindfoot describe cartilage within less accurate constitutive formulations, limiting the description of the mechanical response in the range of linear elastic, homogenous and isotropic materials [23]–[27]. In addition, in solid modeling of complex regions of the foot, the cartilaginous tissue is often considered as fulfilling unique solid between the two bone heads. The two different cartilaginous layers composing the joint are not considered [23]–[26] and, when considered, there is no synovial capsule [26].

In order to define the mechanical response of cartilages of the hindfoot, numerical analysis is developed. For this purpose detailed solid models are developed considering two cartilage layers, one for each bone head, and the synovial capsule for each hindfoot joint. Considering the complexity of the anatomical site, it is necessary to choose an adequate constitutive model in order to have reliable numerical results, with a reasonable computational effort and a reliable definition of constitutive parameters, entailing the existence of adequate experimental reference data, as reported in detail in the following.

2. Material and methods

Constitutive model for the cartilage

In the present work, a fiber-reinforced and almost incompressible hyperelastic constitutive model is assumed to describe the mechanical response of the cartilage. The choice is consistent with the large strains attained by the cartilage tissue, the presence of specifically oriented collagen fibers and the high content of liquid phases [14], [28], [29]. Starting from the right Cauchy–Green strain tensor [30]:

$$\mathbf{C} = \mathbf{F}^T\mathbf{F} \tag{1}$$

where $\mathbf{F}$ is the deformation gradient, there is considered the multiplicative decomposition in volume-changing and volume-preserving components

$$\mathbf{C} = J^{2/3}\mathbf{I}\cdot\widetilde{\mathbf{C}} \tag{2}$$

with $\mathbf{I}$ being the second rank unit tensor and J the determinant of the deformation gradient. From the volume-preserving part $\widetilde{\mathbf{C}}$ of the right Cauchy–Green strain tensor the modified invariants are obtained

$$I_1 = \mathrm{tr}(\widetilde{\mathbf{C}}), \quad I_4 = \widetilde{\mathbf{C}} : (\mathbf{n}_0 \otimes \mathbf{n}_0) \tag{3}$$

$\mathbf{n}_0$ being a unit vector defining the local direction of spatially oriented collagen fibers in the un-deformed configuration of the tissue.

The strain energy function [30] W is defined as a sum of two terms, for ground matrix and collagen fibers [29], respectively,

$$\begin{gathered} W = W_m + W_f, \\ W_m = \frac{K_\nu}{2}(J^2 - 1 - 2\ln J) + \frac{\mu}{2}(\widetilde{I}_1 - 3), \\ W_f = \frac{k_1}{2k_2}[\exp(k_2\langle \widetilde{I}_4 - 1\rangle^2) - 1]. \end{gathered} \tag{4}$$

The stress-like parameter K_ν is related to the initial bulk modulus of the ground matrix and the stress-like parameter μ is its initial shear stiffness. The stress-like parameter k_1, and the dimensionless parameter k_2 are related to the mechanical response of the collagen fibers. The use of the ramp function

$$\langle x\rangle = (x + |x|)/2 \tag{5}$$

allows the stiffness contribution of the collagen fibers only in tensile condition to be considered, which is a mechanical behavior consistent with the conformation of the unloaded fibers.

The stress response in terms of the second Piola–Kirchhoff stress tensor is obtained by taking the derivative of (4) with respect to the right Cauchy–Green strain tensor and is split in additive terms related to ground matrix and reinforcing fibers, respectively,

$$\mathbf{S} = 2\frac{\partial W}{\partial \mathbf{C}} = \mathbf{S}_m + \mathbf{S}_f \tag{6}$$

where the two stress tensors $\mathbf{S}_m$ and $\mathbf{S}_f$ are given by

$$\mathbf{S}_m = K_v(J^2-1)\mathbf{C}^{-1} + \mu\left(J^{-2/3}\mathbf{I} - \frac{1}{3}\widetilde{I}_1\mathbf{C}^{-1}\right), \quad (7)$$

$$\mathbf{S}_f = 2k_1(\widetilde{I}_4 - 1)\exp[k_2(\widetilde{I}_4 - 1)^2]$$

$$\times J^{-2/3}\left\{\mathbf{n}_0 \otimes \mathbf{n}_0 - \frac{1}{3}[\mathbf{C} : (\mathbf{n}_0 \otimes \mathbf{n}_0)]\mathbf{C}^{-1}\right\}. \quad (8)$$

According to the use of the ramp function in W_f the term of the second Piola–Kirchhoff stress tensor (8) is considered only in the case the collagen fibers are elongated. The Cauchy stress tensor is then obtained by the second Piola–Kirchhoff stress tensor through a standard push-forward

$$\boldsymbol{\sigma} = J^{-1}\mathbf{F}\mathbf{S}\mathbf{F}^T. \quad (9)$$

The constitutive model assumed for the cartilage is a specific form of a fiber-reinforced hyperelastic formulation [28] implemented in the general purpose Finite Element code ABAQUS® (SIMULIA, Dassault Systemes) that has been adopted for all the analyses of this work.

Constitutive model fitting

The constitutive parameters are fitted on experimental data obtained from *in vitro* indentation tests on bovine cartilage samples taken from the literature [31], having recognized a similarity in the structural conformation of bovine and human cartilage tissues [32]. Indentation tests are particularly suitable to define the mechanical properties of the cartilage because they reproduce well the compressive states induced in the cartilaginous thickness during *in vivo* conditions. Further, the rate of strain applied in the tests considered corresponds to the strain rate of stance loading condition analyzed subsequently. The finite element model developed to mimic the experimental set up [31] is shown in Fig. 1.

The model consists of one fourth of cartilage sample with the shape of a disk 2 mm thick and a plane ended cylindrical indenter with a diameter of 4 mm, as reported in Fig. 1a. A total compressive displacement of 0.6 mm corresponding to a strain of 33% is imposed on the cartilage sample at strain rate of about 0.1 s^{-1}. The contact between indenter and cartilage is considered frictionless. The cartilaginous tissues of the model are characterized with the hyperelastic fiber-reinforced model reported in the previous section. According to the disposition of the collagen fibers the unit vector $\mathbf{n}_0$ is parallel to upper and lower surfaces and locally disposed in radial direction.

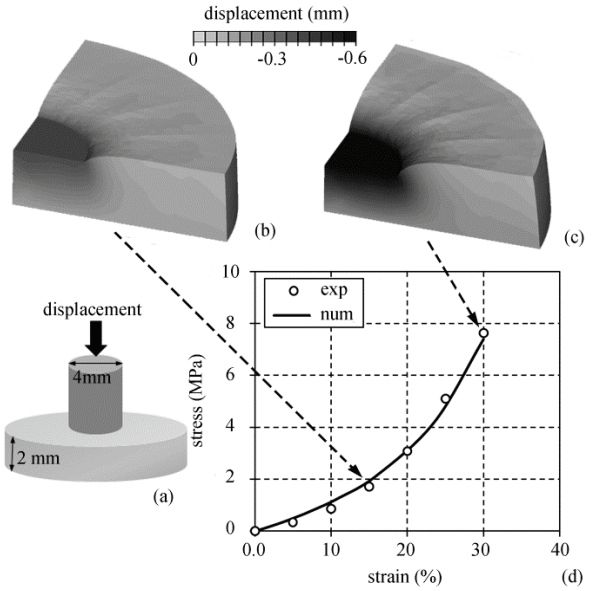

Fig. 1. (a) Representation of experimental [31] loading conditions used to perform the numerical analysis on cartilage samples; (b), (c) contours of the displacement field for 15% and 30% of strain, respectively; (d) comparison between experimental (open circles) and numerical results (continuous lines) as nominal compressive stress (MPa) and nominal strain

The procedure for the definition of the constitutive parameters is based on the minimization of a function [33], [34] estimating the error between experimental data and numerical model results

$$\Omega(\boldsymbol{\alpha}) = \frac{1}{m}\sqrt{\sum_{j=1}^{m}\left[2 - \frac{V_j^{\mathrm{mod}}(\boldsymbol{\alpha}, \lambda_j^{\mathrm{exp}})}{V_j^{\mathrm{exp}}} - \frac{V_j^{\mathrm{exp}}}{V_j^{\mathrm{mod}}(\boldsymbol{\alpha}, \lambda_j^{\mathrm{exp}})}\right]^2} \quad (10)$$

where m is the number of experimental data, λ_j^{exp} the j-th experimental input datum, V_j^{exp} the j-th experimental output datum, V_j^{mod} the j-th numerical model result obtained with the constitutive parameters set $\boldsymbol{\alpha}^i$ and the experimental input λ_j^{exp}. For the case at hand, λ_j^{exp} is the compressive displacement and V_j^{exp}, V_j^{mod} the ratio between force acting on the indenter and contact area of indenter and specimen. The minimization of the function (10) makes use of a stochastic-deterministic procedure [35] to avoid problems arising from the possible existence of local minima.

Numerical analysis

The set of constitutive parameters obtained with the previously described procedure are implemented within the constitutive model adopted for the analysis of the biomechanical behaviour of hindfoot joint. For

this purpose, a specific numerical analysis is developed to interpret *in vivo* experimental tests reported by Li et al. [4] and Wan et al. [36].

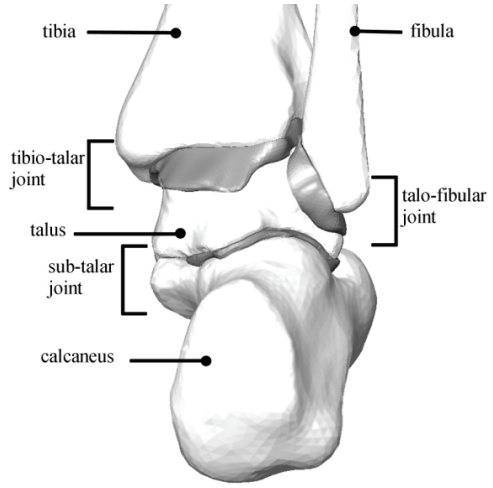

Fig. 2. Solid model of the hind foot, pointing out the regions considered in the numerical model

The solid model of the hindfoot (Fig. 2) is developed with particular attention to the morphometrical aspects of the tibio-talar, sub-talar and talo-fibular joints, considering the sensitivity of numerical results with respect to this aspect. Each joint is modelled with bones, cartilages structures and synovial capsule (Fig. 3). In detail, the models of the bones are developed from TC images of a 58 year old male while cartilages are obtained on the basis of morphometric data from the literature [3], [4], [37]–[40], averaging data pertaining to thickness and mean contact area. The synovial capsule is modelled as a structure enveloping cartilage edges on the basis of anatomical data [41]. The numerical model is obtained by the discretization of the solid model by meshing each hindfoot region with linear tetrahedral elements.

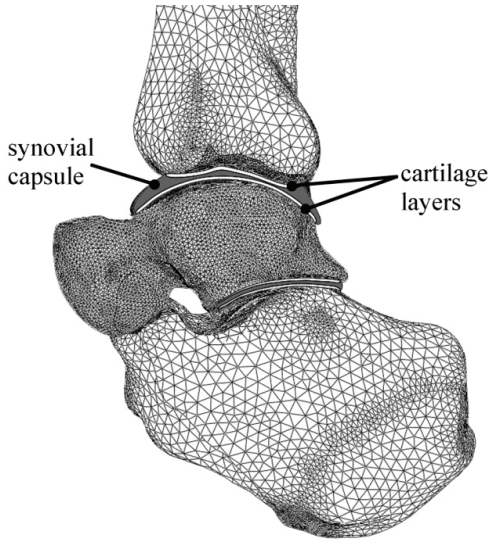

Fig. 3. Numerical model of the hindfoot with details concerning synovial capsule and cartilage layers in the tibio-talar joint

To properly characterise the mechanical properties of each tissue of the hindfoot, specific constitutive formulations are adopted. The cortical portion of the bony segments was assumed to be orthotropic and linearly elastic [41]. The cartilaginous tissue is modelled using the specific fiber-reinforced hyperelastic constitutive model reported above [28], with the set of constitutive parameters given by the fitting obtained through the numerical analysis of the indentation test. The orientations of the collagen fibers are defined by attributing the unit vector $\mathbf{n}_0$ being parallel with respect to the upper surface of the cartilage and radially disposed in the plane of the cartilage. The synovial capsule is characterized as linear elastic and incompressible material [41]–[43], with longitudinal elastic modulus E = 6 MPa.

The experimental tests considered [5], [36] are obtained by non-invasive measurement technique to evaluate the biomechanical behaviour of the tibio-talar joint during a load bearing condition in the stance phase of gait. The procedure uses a dual-orthogonal fluoroscope coupled with MR-images. The experimental set up has incorporated into the fluoroscopic system a force plate to measure ground reaction forces during the test. A series of ankle solid models is defined and the relative position and distance between tibia and talus during stance configuration are measured, making it possible to deduce the variation in thickness of the articular cartilage. In order to interpret the in vivo experimental set-up, the boundary conditions in the numerical model include a load of 765 N along the longitudinal axis of the tibia.

3. Results

The results of the numerical analysis concerning the indentation test are reported in Fig. 1. The contours of the displacement along the longitudinal axis of the indenter are reported in Fig. 1b and Fig. 1c. The numerical results display the cartilage response for different indentation levels. The contact region between the indenter and the cartilage disk layer evolves during the test involving the deformation of the peripheral area of the sample. The constitutive parameters are defined minimizing the discrepancy between indentation experimental data [31] and numerical results (Fig. 1d). The comparison between numerical and experimental data is reported in terms of nominal stress versus nominal strain. Nominal stress is calcu-

lated as the reaction force at the indenter divided by its transversal area, while nominal strain along the thickness of the sample is deduced from the displacement of the indenter divided by the initial thickness. The optimal parameters obtained by the fitting and assumed for describing the biomechanical behavior of articular cartilages are K_v = 9.09 MPa, μ = 0.02 MPa, k_1 = 33.0 MPa and k_2 = 2.1.

These constitutive parameters are adopted when evaluating the biomechanical response of hindfoot cartilaginous tissue during the stance phase of gait. For this purpose, numerical analyses that interpret *in vivo* experimental test [5] are performed. The comparison between *in vivo* experimental data and numerical results obtained in this simulation is represented in Fig. 4.

The graph (Fig. 4a) reports the nominal strain evaluated at the positions indicated by black dots in the cartilage of the talus (Fig. 4b). The representation focuses on the area where the strain assumes the highest intensity and, in agreement with the range of values reported in literature [36], the maximum strain value is 30% at 5 mm of distance from the lateral surface of the talar dome. A transversal section of hindfoot joints (Fig. 5) is considered with more detail and the strain within the articular cartilage is reported.

In order to give a more complete description of the results obtained on tibio-talar cartilages during the stance phase, the contours of the strain field on each layer of the tibio-talar cartilage are illustrated (Fig. 6). Similarly, the strain field contours are reported for the

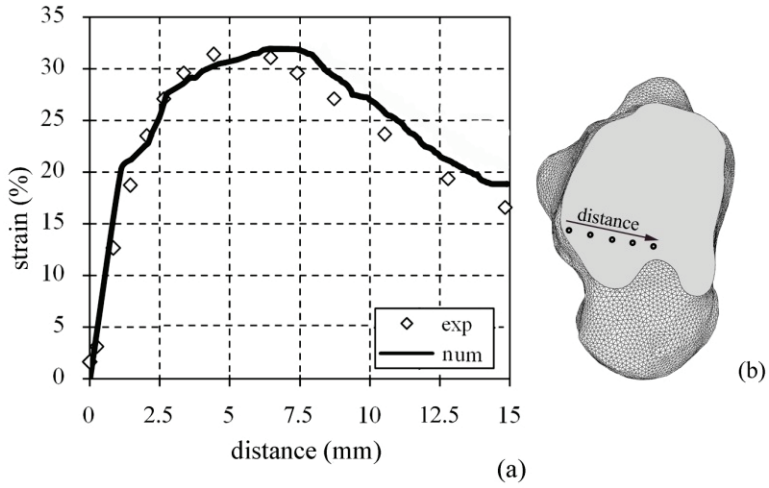

Fig. 4. Comparison between *in vivo* experimental data and numerical results (a) evaluated at the positions indicated by black dots in the cartilage of the talus (b)

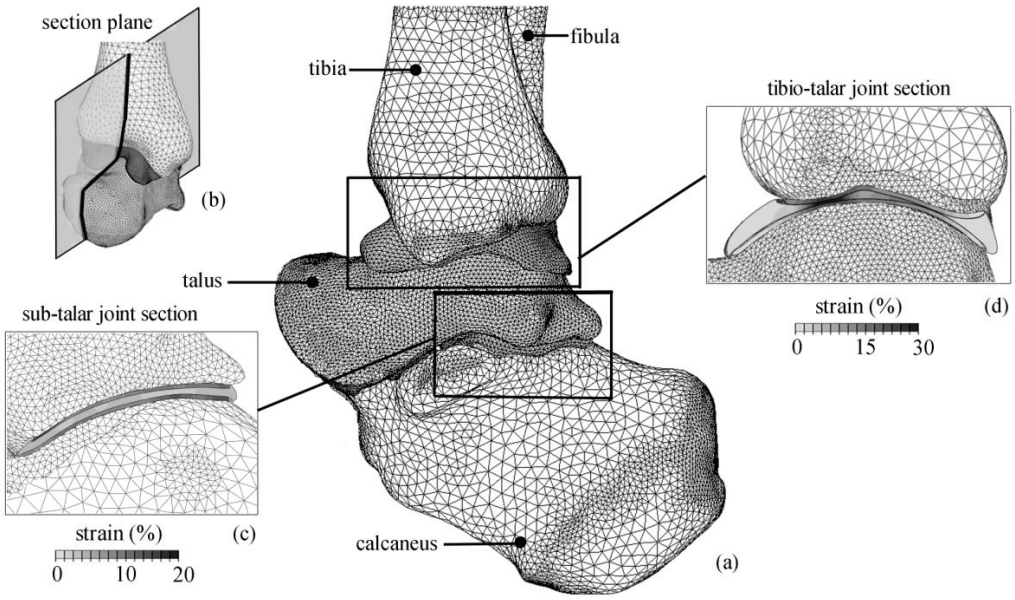

Fig. 5. Numerical model of the hindfoot (a). Contours of the strain field on a transversal section (b) of the sub-talar (c) and tibio-talar joint (d)

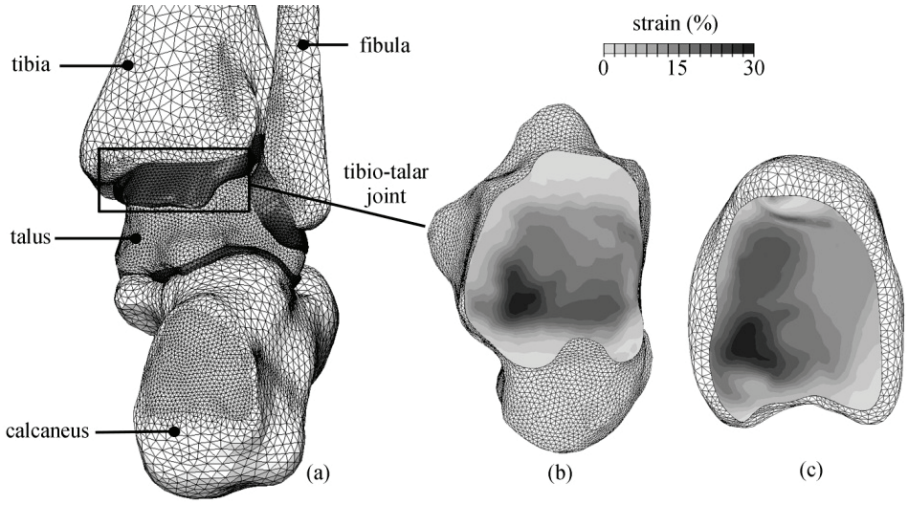

Fig. 6. Numerical model of the hindfoot (a): contours of the strain field on internal surfaces of cartilage of the tibio-talar joint: (b) talar and (c) tibial surfaces

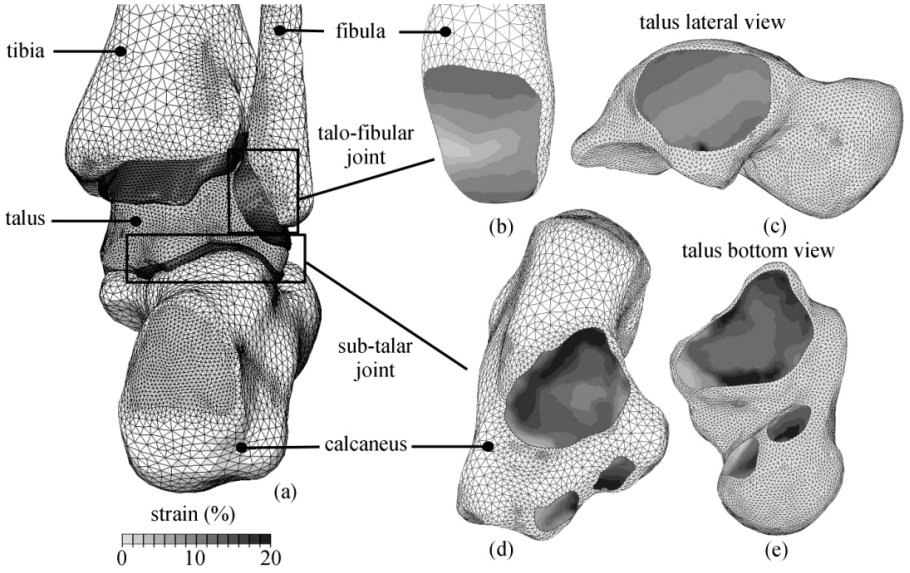

Fig. 7. Numerical model of the hindfoot (a); contours of the strain field on internal surfaces of cartilage of the talo-fibular (b) and (c) and sub-talar (d) and (e) joints, reported on cartilage surfaces of fibula (b), calcaneus (d) and talus (c), (e)

talo-fibular (Fig. 7b and 7c) and sub-talar joint (Fig. 7d and 7e). It is noted that in this condition the maximum value of compressive strain reached in the cartilaginous layers of these joints is about 20%.

4. Discussion

Results from numerical analyses show a good agreement with experimental data from *in vitro* and *in vivo* tests, in particular with the compressive strain field in the cartilage obtained by the analyses of *in vivo* conditions [36]. The maximum compressive stress corresponding to the peak strain is about 3 MPa. This value appears to be consistent with physiological range and under the damage level. In fact, contact stresses in healthy joints typically range from 1 to 6 MPa for light to moderate daily activity [44], while higher stresses are experienced only in localized regions [45], [46]. Moreover, it was found that repetitive compressive stresses of 6.9 MPa are sufficient to produce accelerated fissuring in plugs of articular cartilage and subchondral bone [47].

In the literature several refined constitutive models are proposed for the mechanics of articular cartilage. However, to describe the mechanical behaviour considering an accurate morphological representation and physiological loading, the refinement of the constitutive models adopted is reduced and sometimes the

general complexity of the numerical models induces up to characterize cartilage tissue as linear elastic material [44], [48]. In the present work, within the evaluation of a complete hindfoot three-dimensional model, cartilages are described by using a fiber-reinforced hyperelastic constitutive model, therefore taking into account geometric and material non linear behaviour and anisotropic response due to the collagen fibers contribution. This constitutive model was already considered for its general reliability [50], but not adopted in numerical analyses of a complete ankle joint. Both experimental tests modelled are characterized by the same strain rate (30% s^{-1}) and are consequently adopted within the numerical analysis.

The description of the mechanical response of the cartilage could be refined by considering more complex models that can take into account, for example, the presence of free water to flow in fibers net [14]–[20], or even the inter-molecular forces due to negative and positive charges in a fiber-reinforced poro-viscoelastic swelling model [18], [19]. The adoption of these models would increase the complexity of the numerical approach not only because of the definition of the constitutive parameters set, but also because of the definition of boundary conditions and, in general, must be in direct relationship with experimental data for reliability evaluation. On the other hand, the interest of this work is addressed to the estimation of the maximum compression of the cartilage in the loading phase and proved to be adequate for the purpose.

The numerical model developed in this work includes a cartilage layer juxtaposed on each bone surface of the joint and a region mimicking the synovial capsule with synovial fluid. This can represent an improvement with respect to previous three-dimensional numerical models for the foot reported in literature that do not consider a realistic structural model of hyaline cartilages and synovial capsules. Often articular cartilages are reproduced as homogeneous region simulating the articular connection between the two bone heads. In other cases the mechanical connection is simply described as direct interaction between cartilage surfaces [24]. Within the procedure to account for the effects of the synovial region, the present model has been preliminarily compared with a simplified model where the synovial was not included, as sensitivity analysis. In the latter case, the peak of compressive strain shows to be confined in a much smaller region of the cartilage not compatible with physiological observation, as reported in the literature [51].

Discrepancies between model and *in vivo* experimental data can be caused by morphological differences due to inter-subject variability. Several studies demonstrate that inter-subject variability can be considerably high as far as volume, mean thickness and joint surface [2] of hindfoot cartilage and talus morphology [51] are concerned. In particular, there is emphasized the difference between medial and lateral edges of talus along the coronal plane, which is the medial-lateral line considered in the comparison between numerical analysis experimental data [36]. The cartilages of the tibiotalar joint model are developed considering the specific anatomical conformation, reporting values between 0.67–1.63 mm and 0.4–2.1 mm, respectively, recalling data from literature [2], [3], [36]–[40], [52]–[55]. These considerations stress the necessity of using more extended experimental data.

5. Conclusion

A procedure to investigate articular cartilage from a biomechanical point of view and with regard to the action during the stance phase of the gait is proposed. In particular, attention is focused on hindfoot joints for the important role paid. The comparison between experimental data and numerical results leads to the conclusion that the constitutive model developed is able to offer a proper interpretation of the problem, accounting for typical features of the mechanical behavior of cartilaginous tissue, such as non-linear elasticity, almost-incompressible behaviour and anisotropy.

The numerical analysis pertains to a load representing the effects of weight of a subject in stance configuration. In future development of the present work, more general loading conditions will be assumed, for example, to interpret different physiological configurations such as dorsiflexion, plantar flexion, inversion and eversion, that induce more intense stress and strain states in the cartilage. Moreover, time dependent response will be evaluated, in consideration of effects induced during gate cycle, pointing out characteristic aspects related to strain rate dependency. In addition, the procedure developed for the constitutive modelling of healthy cartilage will be extended to osteoarthritic cartilage. This extension is aimed to evaluate possible mechanical effects related to degraded conditions of the cartilage tissue, facing biomechanical problems that prove to be relevant for their social and economic impact.

References

[1] WIERZCHOLSKI K., *Friction force and pressure calculations for time-dependent impulsive intelligent lubrication of human hip joint*, Acta Bioeng. Biomech., 2010, 12(3), 95–101.

[2] HENDREN L., BEESON P., *A review of the differences between normal and osteoarthritis articular cartilage in human knee and ankle joint*. The Foot, 2010, 19(3), 171–176.

[3] AL-ALI D., GRAICHEN H., FABER S., ENGLMEIER K.H., REISER M., ECKSTEIN F., *Quantitative cartilage imaging of the human hind foot: precision and inter-subject variability*, J. Orthop. Res., 2002, 20(2), 249–56.

[4] ATHANASIOU K.A., LIU G.T., LAVERY L.A., LANCTOT D.R., SCHENCK R.C., *Biomechanical topography of human articular cartilage in the first metatarso-phalangeal joint*, Clin. Orthop. Relat. Res., 1998, 348, 269–281.

[5] LI G., WAN L., KOZANEK M. *Determination of real-time in-vivo cartilage contact deformation in the ankle joint*, J. Biomech., 2008, 41(1), 128–136.

[6] WIERZCHOLSKI K., *Stochastic impulsive pressure calculations for time dependent human hip joint lubrication*, Acta Bioeng. Biomech., 2012, 14(4), 81–100.

[7] CHIZHIK S.A., WIERZCHOLSKI K., TRUSHKO A.V., ZHYTKOVA M.A., MISZCZAK A., *Properties of Cartilage on Micro- and Nano-level*, Adv. in Trib., 2010, ID 243150, 8 pp.

[8] SCHURZ J., RIBITSCH V., *Rheology of synovial fluid*, Biorheol., 1987, 24, 385–399.

[9] BURSAC P.M., OBITZ T.W., EISENBERG S.R., STAMENOVIC D., *Confined and unconfined stress relaxation of cartilage: appropriateness of a transversely isotropic analysis*, J. Biomech., 1999, 32, 1125–1130.

[10] PRENDERGAST P.J., VAN DRIEL W.D., KUIPER J.H., *A comparison of finite element codes for the solution of biphasic poroelastic problems*, Proc. Inst. Mech. Eng., 1996, 210(2), 131–136.

[11] STUEBNER M., HAIDER M.A., *A fast quadrature-based numerical method for the continuous spectrum biphasic poro-viscoelastic model of articular cartilage*, J. Biomech., 2010, 43, 1835–1839.

[12] HAIDER M.A., SCHUGART R.C., *A numerical method for the continuous spectrum biphasic poro-visco-elastic model of articular cartilage*, J. Biomech., 2006, 39, 77–183.

[13] DISILVESTRO M.R., JUN-KYO F.S., *A cross-validation of the biphasic poroviscoelastic model of articular cartilage in unconfined compression, indentation, and confined compression*, J. Biomech., 2001a, 34, 519–525.

[14] LI L.P. , M.D. BUSCHMANN, A. SHIRAZI-ADL, *A fibril reinforced non homogeneous poroelastic model for articular cartilage: inhomogeneous response in unconfined compression*, J. Biomech., 2000, 33, 1533–1541.

[15] GUPTAA S., LINB J., ASHBYC P., PRUITT L., *A fiber reinforced poroelastic model of nanoindentation of porcine costal cartilage: A combined experimental and finite element approach*, J. Mech. Behav. Biomed. Mater., 2009, 2(4), 326–37.

[16] LI L.P., SHIRAZI-ADL A., BUSCHMANN M.D., *Investigation of mechanical behaviour of articular cartilage by fibril reinforced poroelastic models*, Biorheology, 2003, 40, 227–233.

[17] SEIFZADEH A., OGUAMANAM D.C.D., TRUTIAK N., HURTIG M., PAPINI M., *Determination of nonlinear fiber-reinforced biphasic poroviscoelastic constitutive parameters of articular cartilage using stress relaxation indentation testing and an optimizing finite element analysis*, Comput. Methods Programs Biomed., 2012, 107(2), 315–326.

[18] GARCÍA J.J., CORTÉS D.H., *A biphasic viscohyperelastic fibril-reinforced model for articular cartilage: Formulation and comparison with experimental data*, J. Biomech., 2007, 40(8), 1737–1744.

[19] WILSON W., VAN DONKELAAR C.C., VAN RIETBERGEN B., HUISKES R., *A fibril-reinforced poro-viscoelastic swelling model for articular cartilage*, J. Biomech., 2005, 38(6), 1195–1204.

[20] JULKUNEN P., WILSON W., JURVELIN J.S., RIEPPO J., QU C.-J, LAMMI M.J., KORHONEN R.K., *Stress–relaxation of human patellar articular cartilage in unconfined compression: prediction of mechanical response by tissue composition and structure*, J. Biomech., 2008, 41, 1978–1986.

[21] GARCÍA J.J., CORTÉS D.H., *A biphasic visco-hyperelastic fibril-reinforced model for articular cartilage: formulation and comparison with experimental data*, J Biomech., 2007, 40(8), 1737–1744.

[22] DISILVESTRO M.R., SUH J-K F., *A cross-validation of the biphasic poro-viscoelastic model of articular cartilage in unconfined compression, indentation, and confined compression*, J. Biomech., 2001, 34, 519–525.

[23] GEFEN A., *Stress analysis of the standing foot following surgical plantar fascia release*, J. Biomech., 2002, 35(5), 629–637.

[24] CHEUNG J.T.M., ZHANG M., LEUNGA A.K.L., FAN J.B., *Three-dimensional finite element analysis of the foot during standing - a material sensitivity study*, J. Biomech., 2005, 38, 1045–1054.

[25] CHEN W.P., JU C.W., TANG F.T., *Effects of total contact insoles on the plantar stress redistribution: a finite element analysis*, Clin. Biomech., 2003, 18, S17–S24.

[26] ANTUNES P.J., DIAS G.R., COELHO A.T., REBELO F., PEREIRA T., *Non-linear finite element modelling of anatomically detailed 3D foot model*, http://www.materialise.com. 2010.

[27] ANDERSON D.D., GOLDSWORTHY J.K., LI W., JAMES RUDERT M., TOCHIGI Y., BROWN T., *Physical Validation of a Patient-Specific Contact Finite Element Model of the Ankle*, J. Biomech., 2007, 40(8), 1662–1669.

[28] LI L.P., BUSCHMANN M.D., SHIRAZI-ADL A., *Strain-rate dependent stiffness of articular cartilage in unconfined compression*, J. Biomech. Eng., 2003, 125(2), 161–168.

[29] WEISS J.A., MAKER B.N., GOVINDJE S., *Finite element implementation of incompressible, transversely isotropic hyperelasticity*, Comput. Meth. Appl. Mech. Eng., 1996, 135(1–2), 107–128.

[30] MARSDEN J.E., HUGHES T.J.R., *Mathematical Foundations of Elasticity*, Dover Publications, New York, 1994.

[31] BROWN C.P., CRAWFORD R.W., OLOYEDE A., *Indentation stiffness does not discriminate between normal and degraded articular cartilage*, Clin. Biomech., 2007, 22(7), 843–848.

[32] ATHANASIOU K.A., ROSENWASSER M.P., BUCKWALTER J.A., MALININ T.I., MOW V.C., *Interspecies comparison of in situ intrinsic mechanical properties of distal femoral cartilage*, J. Orthop. Res., 1991, 9, 330–340.

[33] FORESTIERO A., CARNIEL E.L., NATALI A.N., *Biomechanical behaviour of ankle ligaments: constitutive formulation and numerical modelling*, Comp. Meth. Biomech. Biomed. Eng., in press; DOI: 10.1080/10255842.2012.688105.

[34] NATALI A.N., FONTANELLA C.G., CARNIEL E.L., YOUNG J.M., *Biomechanical behaviour of heel pad tissue: experimental testing, constitutive formulation, and numerical modelling*, P. I. Mech. Eng. H, 2011, 225, 449–459.

[35] NATALI A.N., FORESTIERO A., CARNIEL E.L., *Parameters identification in constitutive models for soft tissues mechanics*, Russ. J. Biomech., 2009, 4(46), 29–39.

[36] WAN L., DE ASLA R.J., RUBASH H.E., LI G., *Determination of in-vivo articular cartilage contact areas of human talocrural*

joint under weight-bearing conditions, Osteoarthritis and Cartilage, 2006, 14(12), 1294–1301.

[37] WELSCH G.H., MAMISCH T.C., HUGHES T., ZILKENS C., QUIRBACH S., SCHEFFLER K., KRAFF O., SCHWEITZER M.E., SZOMOLANYI P., TRATTNIG S., *In vivo biochemical 7.0 Tesla magnetic resonance: preliminary results of d-GEMRIC, zonal T2, and T2 mapping of articular cartilage*, Invest. Radiol., 2008, 43(9), 619–626.

[38] MILLINGTON S.A., GRABNER M., WOZELKA R., ANDERSON D.D., HURWITZ S.R., CRANDALL J.R., *Quantification of ankle articular cartilage topography and thickness using a high resolution stereophotography system*, Osteoarthritis Cartilage, 2007, 15, 205–211.

[39] SUGIMOTO K., TAKAKURA Y., TOHNO Y., KUMAI T., KAWATE K., KADONO K., *Cartilage thickness of the talar dome*, Arthroscopy, 2005, 21(4), 401–404.

[40] ADAM C., ECKSTEIN F., MILZ S., PUTZ R., *The distribution of cartilage thickness within the joints of the lower limb of elderly individuals*, J. Anat., 1998, 193, 203–214.

[41] SAFARI M., BJELLE A., GUDMUNDSSON M., HÖGFORS C., GRANHED H., *Clinical assessment of rheumatic diseases using viscoelastic parameters for synovial fluid*, Biorheol., 1990, 27(5), 659–74.

[42] QUYNHHOA T.N., WONGA B.L., CHUN J., YOON Y.C., TALKE F.E., SAH RL., *Macroscopic assessment of cartilage shear: Effects of counter-surface roughness, synovial fluid lubricant, and compression offset*, J Biomech., 2010, 43, 1787–1793.

[43] FAM H., BRYANT J.T., KONTOPOULOU M., *Rheological properties of synovial fluids*, Biorheol., 2007, 44(2), 59–74.

[44] NATALI A.N., FORESTIERO A., CARNIEL E.L., PAVAN P.G., DAL ZOVO C., *Investigation of foot plantar pressure: experimental and numerical analysis*, Med. Biol. Eng. Comput., 2010, 48, 1167–1174.

[45] MÜLLER-GERBL M., PUTZ R., *Demonstration of subchondral bone density patterns by three-dimensional CT osteo absorptiometry as a non-invasive method for in vivo assessment of individual long-term stresses in joints*, J. Bone and Mineral Res., 1992. S411–S418.

[46] PARK S., NICOLL S.B., MAUCK R.L., ATESHIAN G.A., *Cartilage mechanical response under dynamic compression at physiological stress levels following collagenase digestion*, Ann. Biomed. Eng., 2008, 36(3), 425–434.

[47] REPO R.U., FINLAY J.B., *Survival of articular cartilage after controlled impact*, Journal of Bone and Joint Surgery [Am], 1977, 59-A, 1068–1076.

[48] ZIMMERMAN N.B., SMITH D.G., POTTENGER L.A., COOPERMAN D.R., *Mechanical disruption of human patellar cartilage by repetitive loading in vitro*, Clin. Orthop. Relat. Res., 1988, (229), 302–307.

[49] CHEN W.M., LEE T., LEE P.V.S., LEE J.W., LEE S.J., *Effects of internal stress concentrations in plantar soft-tissue A preliminary three-dimensional finite element analysis*, Med. Eng. Phys., 2010, 32(4), 324–331.

[50] BROWN C.P., NGUYEN T.C., MOODY H.R., CRAWFORD R.W., OLOYEDE A., *Assessment of common hyperelastic constitutive equations for describing normal and osteoarthritic articular cartilage*, Proc. Inst. Mech. Eng. H., 2009, 223(6), 643–652.

[51] ANDERSON D.D., GOLDSWORTHY J.K., SHIVANNA K., GROSLAND N.M., PEDERSEN D.R., THOMAS T.P., TOCHIGI Y., MARSH J.L., RUDERT M.J., BROWN T.D., *Intra-articular Contact Stress Distributions at the Ankle throughout Stance Phase – Patient-Specific Finite Element Analysis as a Metric of Degeneration Propensity*, J. Biomech., 2007, 40(8), 1662–1669.

[52] WIEWIORSKI M., HOECHEL S., WISHART K., LEUMANN A., MÜLLER-GERBL M., VALDERRABANO V., NOWAKOWSKI A.M., *Computer Tomographic Evaluation of Talar Edge Configuration for Osteochondral Graft Transplantation*, Clin. Anat., 2012, 25(6), 773–780.

[53] EL-KHOURY G.Y., ALLIMAN K.J., LUNDBERG H.J., RUDERT M.J., BROWN T.D., SALTZMAN C.L., *Cartilage Thickness in Cadaveric Ankles: Measurement with Double-Contrast Multi–Detector Row CT Arthrography versus MR Imaging*, Radiol., 2004, 233, 768–773.

[54] KUETTNER K.E., COLE A.A., *Cartilage degeneration in different human joints*, Osteoarth. Cart., 2005, 13(2), 93–103.

[55] SHEPHERD D.E.T., SEEDHOM B.B., *Thickness of human articular cartilage in joints of the lower limb*, Ann. Rheum. Dis., 1999, 58, 27–34.